CO31: Structure of white dwarf stars

Lyubomir Shoylev, shil5377
lyubomir.shoylev@st-hildas.ox.ac.uk
St Hilda's College
February 20, 2021

Abstract

This will be the abstract of the report. It shall be written when the rest is nearly done.

1 Introduction

The goal of this experiment is to study the internal structure of white dwarf stars. They are one possible end state in the life cycle of stars. What is particular about white dwarf stars is that the matter they are composed of is different from the matter in a usual star similar to the Sun. While in a usual stable star the equilibrium is supported by fusion energy and the pressure of the plasma, a white dwarf star has exhausted its fuel, and the equilibrium is supported by electron degeneracy pressure, making the star extremely dense; for example, a white dwarf of 1 solar mass is about the size of Earth. In this report, we will first derive the coupled differential equations for mass and density in a spirit similar to Oxford Physics (2020) and Chandrasekhar (1984) in Section 2. Then, in Section 3, we develop the numerical method used to solve the coupled equations. Results and discussion take place in Section 4. Finally, we give a summary of the experiment and possible improvements in Section 5.

2 Theory of white dwarf stars

Stars are astronomical objects with ellipsoid shape made up of heated plasma. The force of gravity tries to compress the ball, holding the matter together, while the gaseous plasma opposes gravity with the pressure it exerts. When the two forces balance each other out, the star is in hydrostatic equilibrium. In usual stars, pressure is due to the gas and the radiation (which becomes important mostly in the largest non-degenerate stars). In white dwarf stars, however, the densities are far greater than the ones found in usual stars, and matter behaves differently. All electrons are no longer bound to atoms and are free to roam. The behaviour can approximately be modelled by a Fermi gas of electrons at zero Kelvin (i.e. fully degenerate state). Hence, the pressure ensuring the equilibrium is the degeneracy pressure of the electrons.

2.1 Equation of equilibrium

Assume the star is spherically symmetric, in equilibrium, non-rotating, and the effect of magnetic fields is negligible. Therefore, all properties depend only on the distance to the centre of the star, r. The gravitational force on a small volume of matter with area $\mathrm{d}A$ and radial height $\mathrm{d}r$ is:

$$F_{\mathrm{G}} = -\frac{Gm\left(r\right)\mathrm{d}m}{r^2}, \tag{1}$$

where $m\left(r\right)$ is the mass of the star contained up to r, $\mathrm{d}m = \mathrm{d}A\,\mathrm{d}r\rho\left(r\right)$ is the mass of the small volume, and the density $\rho\left(r\right)$ was assumed constant (negative sign because it pulls towards the centre). The force due to the pressure is the difference of the forces at r and $r + \mathrm{d}r$:

$$F_{\mathrm{P}} = \left(P\left(r\right) - P\left(r + \mathrm{d}r\right)\right)\mathrm{d}A. \tag{2}$$

For a star in equilibrium the two forces balance eachother out, i.e. $F_{\mathrm{G}} + F_{\mathrm{P}} = 0$. After rearranging, we get:

$$\frac{\mathrm{d}P(r)}{\mathrm{d}r} = \frac{P\left(r + \mathrm{d}r\right) - P\left(r\right)}{\mathrm{d}r} = -\frac{G\rho(r)m(r)}{r^2}. \tag{3}$$

We can rewrite the hydrostatic equilibrium by using the chain rule:

$$\frac{\mathrm{d}P(r)}{\mathrm{d}r} = \frac{\mathrm{d}P}{\mathrm{d}\rho}\frac{\mathrm{d}\rho}{\mathrm{d}r}, \tag{4}$$

so equation (3) becomes:

$$\frac{\mathrm{d}\rho}{\mathrm{d}r} = -\frac{\mathrm{d}\rho}{\mathrm{d}P}\frac{G\rho(r)m(r)}{r^2}. \tag{5}$$

On the other hand, the equation for the inscribed mass is:

$$m(r) = \int_0^r \mathrm{d}r' 4\pi^2 r' \rho\left(r'\right) \quad \Rightarrow \quad \frac{\mathrm{d}m}{\mathrm{d}r} = 4\pi r^2 \rho(r) \tag{6}$$

We are now left with two coupled differential equations, (5) and (6). The last task before obtaining the full equation is to determine $\frac{\mathrm{d}P}{\mathrm{d}\rho}$, which depends on the equation of state.

2.2 Equation of state

We assume the star is made up primarily of heavy ^{56}Fe nuclei and their electrons. The nuclei carry most of the mass and little of the pressure, while the opposite is true for the electrons. Since *very high* densities are considered, we can approximate that the nuclei are stationary while the electrons move freely, not bound to any nuclei. A good model for the freely moving electron gas is the free Fermi gas at $T = 0\,\mathrm{K}$. This is the fully degenerate state, in which electrons fill all energy (momentum) levels up to the Fermi energy (momentum).

Fermions obey the Pauli exclusion principle, therefore each energy level is $2S+1$ degenerate, where $S = \frac{1}{2}$ in the case of electrons. This degeneracy factor multiplies gives the density function:

$$g(k) = \frac{2S+1}{2\pi^2} V k^2, \tag{7}$$

where k is the wavevector of particles and V is the volume of the system. The number density of particles can therefore be written as:

$$n = \frac{N}{V} = \frac{1}{V}\int_0^{k_\mathrm{F}} \mathrm{d}k\, g(k) = \int_0^{k_\mathrm{F}} \mathrm{d}k \frac{2S+1}{2\pi^2} k^2. \tag{8}$$

Here we integrate up to k_F where this is given by $p_\mathrm{F} = \hbar k_\mathrm{F}$ and p_F is the Fermi momentum. Rewrite the above equation in terms of p:

$$n = \int_0^{p_\mathrm{F}} \mathrm{d}p \frac{2S+1}{2\pi^2\hbar^3} p^2 = \int_0^{p_\mathrm{F}} \mathrm{d}p \frac{8\pi}{h^3} p^2 = \int_0^{p_\mathrm{F}} \mathrm{d}p\, n(p) = \frac{m_\mathrm{e} 8\pi}{h^3} p_\mathrm{F}^3 \tag{9}$$

where we define $n(p)\,\mathrm{d}p$ as the number of electrons per unit volume with momentum between p and $p + \mathrm{d}p$.

Pressure, on the other hand, is given by the kinetic expression:

$$P = \frac{1}{3}\int_0^{p_\mathrm{F}} p v_p n(p)\,\mathrm{d}p. \tag{10}$$

At this point we need to differentiate between non-relativistic and relativistic cases - v_p has a different value in the two cases:

$$v_p = \begin{cases} \frac{p}{m_\mathrm{e}} & \text{in the non-relativistic case} \\ \frac{pc^2}{\sqrt{p^2c^2 + m_\mathrm{e}^2 c^4}} & \text{in the relativistic case} \end{cases}. \tag{11}$$

Let us first work out the answer in the non-relativistic case. The integral becomes const $\times \int p^4\,\mathrm{d}p$, so the pressure becomes:

$$P_\mathrm{non} = \frac{8\pi}{15h^3 m_\mathrm{e}} p_\mathrm{F}^5. \tag{12}$$

For the relativistic case, rather than do the integral for P involving hyperbolic functions, differentiaite (10) by parts:

$$\frac{\mathrm{d}P_\mathrm{rel}}{\mathrm{d}\rho} = \frac{\mathrm{d}P_\mathrm{rel}}{\mathrm{d}p_\mathrm{F}}\frac{\mathrm{d}p_\mathrm{F}}{\mathrm{d}\rho}, \quad \frac{\mathrm{d}P_\mathrm{rel}}{\mathrm{d}p_\mathrm{F}} = \frac{8\pi}{3h^3}\frac{\mathrm{d}}{\mathrm{d}p_\mathrm{F}}\int_0^{p_\mathrm{F}} \frac{p^4c^2}{\sqrt{p^2c^2 + m_\mathrm{e}^2c^4}}\,\mathrm{d}p = \frac{8\pi}{3h^3}\frac{p_\mathrm{F}^4 c}{\sqrt{p_\mathrm{F}^2c^2 + m_\mathrm{e}^2c^4}}. \tag{13}$$

We can collect the derivative of (12) and the result of (13):

$$\frac{\mathrm{d}P}{\mathrm{d}\rho} = \frac{\mathrm{d}p_\mathrm{F}}{\mathrm{d}\rho}\frac{8\pi}{3h^3 m_\mathrm{e}} p_\mathrm{F}^4 \begin{cases} 1 & \text{in the non-relativistic case} \\ \left(1 + \frac{p_\mathrm{F}^2}{m_\mathrm{e}^2 c^2}\right)^{-1/2} & \text{in the relativistic case} \end{cases}. \tag{14}$$

What is left is expressing $p_{\mathrm{F}}(\rho)$ to complete the equation of state in the form needed by (5). The relation between density and number density can be stated as $\rho = \mu_{\mathrm{e}} m_{\mathrm{p}} n$, where μ_{e} is the mean molecular weight per electron and m_{p} is the mass of 1 proton. In our case, we can approximate $\mu_{\mathrm{e}} \approx 2$. Using this relation and (9), we arrive at:

$$p_{\mathrm{F}} = \left(\frac{h^3}{8\pi} n\right)^{1/3} = \left(\frac{h^3}{16\pi m_{\mathrm{p}}} \rho\right)^{1/3} \quad \Rightarrow \quad \frac{\mathrm{d}p_{\mathrm{F}}}{\mathrm{d}\rho} = \frac{1}{3}\left(\frac{h^3}{16\pi m_{\mathrm{p}}}\right)^{1/3} \rho^{-2/3} \tag{15}$$

2.3 The limiting mass

The limiting case of ultra-relativistic electrons can be obtained by setting $v_p = c$ (i.e. taking the limit $pc \gg m_{\mathrm{e}} c^2$) in (10) to arrive at the equation of state:

$$P_{\mathrm{ultra}} = \frac{p\pi}{3h^3} \int_0^{p_{\mathrm{F}}} p^3 c \, \mathrm{d}p = \frac{2\pi c}{3h^3} p_{\mathrm{F}}^4. \tag{16}$$

As noted in Chandrasekhar (1984), this leads to a specific equation for the mass with a well specified value $M_{\mathrm{lim}} = 5.76 \mu_{\mathrm{e}}^{-2} M_{\odot}$, where $M_{\odot}$ is one solar mass; this limit is equivalent to infinite mean density and zero radius of the star. In the approximation made above the limiting mass is $M_{\mathrm{lim}} \approx 1.435 M_{\odot}$. We can draw two important conclusions from this fact: first, there is an upper limit to masses of degenerate stars in the later stages of evolution; and second, we cannot predict the end evolutionary state of stars with mass $M > M_{\mathrm{lim}}$ in this physical framework.

3 Numerical approach

To find the radius and mass of the star as a function of its central density, we will numerically integrate the coupled system. The distance r at which $\rho(r = R) \approx 0$ is where the star ends; the mass is therefore $m(R)$ where $m(r)$ is the inscribed mass, as defined in (6). Physically, we can consider solving the equation as an initial value problem. First, write the coupled system in vector form:

$$\boldsymbol{y} = \begin{pmatrix} \rho \\ m \end{pmatrix}, \tag{17}$$

and the derivatives of its members with respect ro r given by (5) and (6). Then, for a given central density ρ_{c} the initial condition for the mass is specified by $m(\delta r) = \frac{4}{3}\pi(\delta r)^3 \rho_{\mathrm{c}}$ for some small distance from the centre δr. The structure of the code and parts of the source can be found in Appendix A.

3.1 Why integration?

Since we have an initial value problem, the underlying idea is the following: rewrite the derivatives as fractions of finite differences, and get $\Delta \boldsymbol{y} = \frac{\mathrm{d}\boldsymbol{y}(x)}{\mathrm{d}x} \Delta x$. This is the change in $\boldsymbol{y}$ when we step through by Δx. When the step is very small, the approximation is very good, i.e. $\lim_{\Delta x \to \mathrm{d}x} \Delta \boldsymbol{y} = \mathrm{d}\boldsymbol{y}$.

The basic idea boils down to the most elementary such method — Euler's method:

$$\begin{aligned} \boldsymbol{y}_{\mathrm{n}+1} &= \boldsymbol{y}_{\mathrm{n}} + h \boldsymbol{f}(x_{\mathrm{n}}, \boldsymbol{y}_{\mathrm{n}}) \\ x_{\mathrm{n}+1} &= x_{\mathrm{n}} + h, \end{aligned} \tag{18}$$

where the vector function is just $\boldsymbol{f} = \frac{\mathrm{d}\boldsymbol{y}(x)}{\mathrm{d}x}$ i.e. the slope at x_{n} and $h = \Delta x$. This is a first order method: the local error is $\sim h^2$ and the global error therefore is $\sim h$. This method has only one computation of the derivative and is therefore very fast, but also very innacurate.

A similar explicit second order method is Heun's method (trapezoid rule):

$$\begin{aligned} \boldsymbol{y}_{\mathrm{n}+1} &= \boldsymbol{y}_{\mathrm{n}} + \frac{1}{2} h \Big(\boldsymbol{f}(x_{\mathrm{n}}, \boldsymbol{y}_{\mathrm{n}}) + \boldsymbol{f}\big(x_{\mathrm{n}} + h, \boldsymbol{y}_{\mathrm{n}} + \boldsymbol{f}(x_{\mathrm{n}}, \boldsymbol{y}_{\mathrm{n}})\big) \Big) \\ x_{\mathrm{n}+1} &= x_{\mathrm{n}} + h, \end{aligned} \tag{19}$$

Here the local error is $\sim h^3$ and the global error therefore is $\sim h^2$.

The method we will later use to compute properties of white dwarf stars is the 4th order Runge-Kutta (RK4) method. It features four evaluations of the derivative and a global error $\sim h^4$, offering a balance between computational time and accuracy. This method takes values for the slope at four different positions and estimates the step

size by weighted average of these four steps. In equations:

$$\begin{aligned}
\boldsymbol{k_1} &= h\boldsymbol{f}(x_\mathrm{n}, \boldsymbol{y}_\mathrm{n}) \\
\boldsymbol{k_2} &= h\boldsymbol{f}\left(x_\mathrm{n} + \frac{1}{2}h, \boldsymbol{y}_\mathrm{n} + \frac{1}{2}\boldsymbol{k_1}\right) \\
\boldsymbol{k_3} &= h\boldsymbol{f}\left(x_\mathrm{n} + \frac{1}{2}h, \boldsymbol{y}_\mathrm{n} + \frac{1}{2}\boldsymbol{k_2}\right) \\
\boldsymbol{k_4} &= h\boldsymbol{f}(x_\mathrm{n} + h, \boldsymbol{y}_\mathrm{n} + \boldsymbol{k_3}).
\end{aligned}$$

Finally, the new position is calculated as:

$$\boldsymbol{y}_{\mathrm{n}+1} = \boldsymbol{y}_\mathrm{n} + \frac{1}{6}\boldsymbol{k_1} + \frac{1}{3}\boldsymbol{k_2} + \frac{1}{3}\boldsymbol{k_3} + \frac{1}{6}\boldsymbol{k_4}. \tag{20}$$

The RK methods family gives approximate solutions to Nth order by varying the weights in the $\boldsymbol{k}$ expressions and the final expression to mathc coefficients in the Taylor expansion.

MENTION STIFF EQUATIONS.

3.2 Comparison of methods

In this section we compare the stability/accuracy of three methods presented in Secction 3.1. For the task, we will try to integrate a solution of the simple harmonic oscillator (SHO), namely:

$$\ddot{x} + \omega^2 x = 0, \qquad \text{with solution} \qquad x = x_0 \cos(\omega t) \tag{21}$$

where we choose $x_0 = 1$ and $\omega = 2\pi$ so the period of oscillations is 1 s. From some initial runs integrating the white dwarf equation we are aware that the number of intervals relevant us is on the order of 10^6 so we choose to compare the two methods on this scale (more discussion on the topic in Section 3.4).

The runs will be split into two groups. The first group is with 10^6 time intervals of length 1 ms for the three methods; denote the results from these runs by Euler1, Heun, and RK4 respectively. The second group is 10^7 time intervals of length 0.1 ms for the Euler method to cover the same total time interval; denote results by Euler2. Additionally, we will consider the energy in the system:

$$E = \frac{\dot{x}^2}{2} + \frac{\omega^2 x^2}{2}. \tag{22}$$

When the method over/underestimates the correction, the effect will build up and change the total energy, which is equivalent to the change in amplitude.

Results are presented in Figure 1. In 1a (first 20 periods of oscillation displayed), we see the calculated position by the three methods Euler1, Euler2, and Heun. It is immediately obvious that Euler1 goes off in the solution pretty quickly. This is confirmed in 1b, where we can have a better look at how the numerical solution deviates from the actual one - Euler1 gains an additional half amplitude in 20 periods, while the other two methods oscillate about zero with Heun having the smaller error. To compare for the whole time of integration and compare these three runs with RK4, plot the relative energy deviation compared to the theoretical value of $2E_0 = \omega^2 \times 1$ on a logarithmic scale. As it can be seen in 1c and 1d, the energy for the first three runs grows exponentially with time after some moment with different exponents, while the fourth run RK4 keeps almost a constant value of energy — the change in energy at $t_0 = 0\,\mathrm{s}$ and $t_1 = 100\,\mathrm{s}$ is:

$$\frac{\left|E(t_1) - E(t_0)\right|}{E(t_0)} \approx 9.755 \cdot 10^{-7}. \tag{23}$$

With these results in mind, we make the obvious choice for a method and continute forwards using the Runge-Kutta 4th order method in all of the following chapters.

3.3 Dimensionless equation for the white dwarf

To calculate values with the computer, we will go to dimensionless quantities in the differential equation. Introduce the following substitutions:

$$\rho = \rho_\mathrm{c}\theta, \quad r = \ell\xi, \quad m = \rho_\mathrm{c}(1\,\mathrm{m}^3)\mu, \text{ therefore } \boldsymbol{y}(r) = \begin{pmatrix}\rho(r)\\ m(r)\end{pmatrix} \to \boldsymbol{\eta}(\xi) = \begin{pmatrix}\theta(\xi)\\ \mu(\xi)\end{pmatrix}. \tag{24}$$

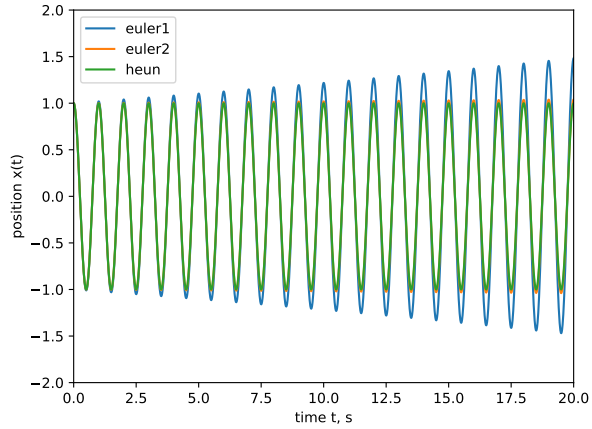

(a) Position as a funcion of time. Notice how eul1 deviates very fast.

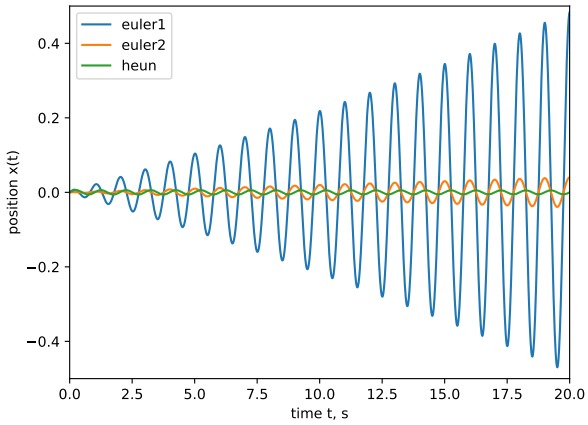

(b) Deviation from the theoretical solution.

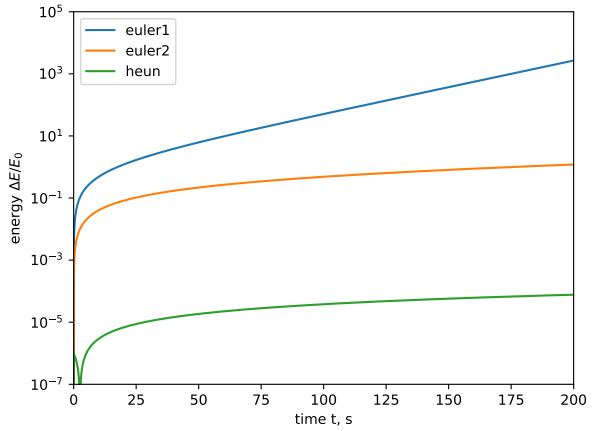

(c) Energy deviation $\Delta E/E_0$ for first three methods.

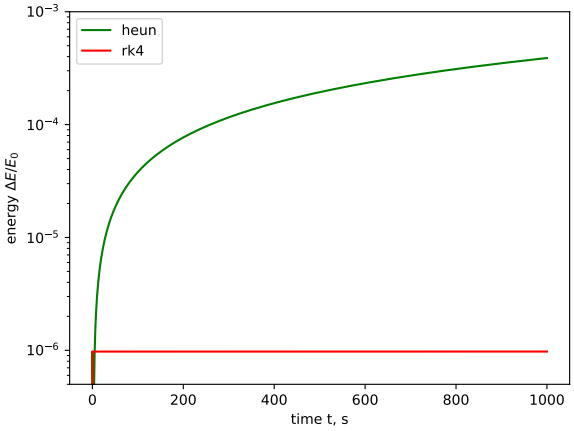

(d) Energy deviation $\Delta E/E_0$ for heun and rk4.

Figure 1: Test runs of SHO integrated with different methods. Blue line is for Euler's method integrated with step $1\,\mathrm{ms}$, yellow line for Euler's method integrated with step $0.1\,\mathrm{ms}$, green line is for Heun's method with step $1\,\mathrm{ms}$, and red line is for RK4 method with step $1\,\mathrm{ms}$.

where we chage variables from $\boldsymbol{y}(r) = \begin{pmatrix}\rho(r)\\ m(r)\end{pmatrix}$ to $\boldsymbol{\eta}(\xi) = \begin{pmatrix}\theta(\xi)\\ \mu(\xi)\end{pmatrix}$. We also specify the length ℓ by the equation $\frac{4}{3}\pi\ell^3 = 1\,\mathrm{m}^3$, which gives a value of $\ell \approx 0.62 \sim 1\,\mathrm{m}$. This will be useful to make some cancelations in the coefficients in the final form of the differential equation for $\boldsymbol{\eta}$.

For (6) the conversion is straightforward:

$$\frac{\rho_\mathrm{c}\,\mathrm{d}\mu}{\ell\,\mathrm{d}\xi} = 4\pi\ell^2\xi^2\rho_\mathrm{c}\theta \quad\Rightarrow\quad \frac{\mathrm{d}\mu}{\mathrm{d}\xi} = 3\xi^2\theta. \tag{25}$$

For the θ equation we have to take into consideration the regime we operate in — whether we solve for a relativistic or non-relativistic equation of state. Firstly, write equations in (15) using the new coordinates we have introduced:

$$p_\mathrm{F} = \left(\frac{h^3\rho_\mathrm{c}}{16\pi m_\mathrm{p}}\right)^{1/3}\theta^{1/3}, \quad \frac{\mathrm{d}p_\mathrm{F}}{\mathrm{d}\rho} = \frac{1}{3}\left(\frac{h^3}{16\pi m_\mathrm{p}\rho_\mathrm{c}^2}\right)^{1/3}\theta^{-2/3}. \tag{26}$$

Now substitute (14) in (5) using (26). After some algebra with the constants, the final result is the following:

$$\frac{\mathrm{d}\theta}{\mathrm{d}\xi} = K_1\frac{\mu\theta^{1/3}}{\xi^2}\begin{cases}1 & \text{in the non-relativistic case}\\ \left(1+K_2\theta^{2/3}\right)^{1/2} & \text{in the relativistic case}\end{cases}, \tag{27}$$

where the constants K_1 and K_2 are given by

$$K_1 = -2^{13/3}\pi \mathrm{G} m_\mathrm{e} m_\mathrm{p}^{5/3} \rho_\mathrm{c}^{1/3} h^{-2}, \qquad K_2 = \frac{1}{m_\mathrm{e}^2 c^2}\left(\frac{3h^3\rho_\mathrm{c}}{16\pi m_\mathrm{p}}\right)^{2/3}. \tag{28}$$

We have completed the task of bringing the equation to normalized coordinates. This is the setup used in writing the code for the white dwarf ODE wrapper presented in A.1

3.4 Convergence and number of intervals

What is left is to choose the coarsness in the grid of ξ. We know that for some $\Delta\xi$ small enough, the answers will converge to $\approx$ a single value. To find the number of intervals (NoI) at which the result converges, we make experimental runs at three different ρ_c — 10^6, 10^{10}, and 10^{14} $\mathrm{kg\,m^3}$ (this spans the range for which we run the experiment later), and test for a NoI in the range $\left\{a \cdot 10^b \mid a \in \{1,2,4,8\}, b \in \{2,3,\dots 8\}\right\}$. The maximal radius is set to $8.1 \cdot 10^7$ in units of ξ, since this turns out to be about the maxium physical radius a white dwarf can be for the range of ρ_c we test. Both the non-relativistic and relativistic cases are considered.

The results are presented in Figure 2. We use the relative error in computed value with respect to the converged value. The latter is estimated as the average of the last three values in the caluclation, i.e. for NoI $2 \cdot 10^8$, $4 \cdot 10^8$, and $8 \cdot 10^8$; the result is $M_\mathrm{conv}, R_\mathrm{conv}$. The relative error is given by:

$$\frac{\Delta M}{M_\mathrm{conv}} = \frac{|M - M_\mathrm{conv}|}{M_\mathrm{conv}}, \quad \frac{\Delta R}{R_\mathrm{conv}} = \frac{|R - R_\mathrm{conv}|}{R_\mathrm{conv}}. \tag{29}$$

What we aim for in our choice for the number of intervals is: on the one side, a low enough number so the computation does not take too long, and on the other side, a high enough number so an acceptable accuracy is achieved. From the logarithmic plots for the mass we can see that the error either goes to zero (the vertical line) or is fixed to $\approx$ zero for NoI $\geq 4 \cdot 10^5$. In the case of the radius determination, we see that the computed value does not really converge to a specific point; it does, however, reduce its error exponentially fast. Let us choose a desired accuracy of below $10^{-5} = 0.001\%$, given that our model is not very accurate. From the logarithmic plots again we see that this is satisfied for NoI $\geq 2 \cdot 10^6$. Therefore, we can use this value as the NoI with a good compromise between speed and accuracy.

4 Results and discussion

5 Summary

this is a citation Sagert et al. (2005)

References

Chandrasekhar, S. (1984), 'On stars, their evolution and their stability', *Reviews of Modern Physics* **56**(2), 137–147.

Oxford Physics (2020), *CO31: Structure of white dwarf stars*, Oxford Physics.

Sagert, I., Hempel, M., Greiner, C. and Schaffner-Bielich, J. (2005), 'Compact stars for undergraduates', *Eur.J.Phys.27:577-610,2006* .

A Source code

A.1 White Dwarf ODE wrapper code

B Derivations of white dwarf

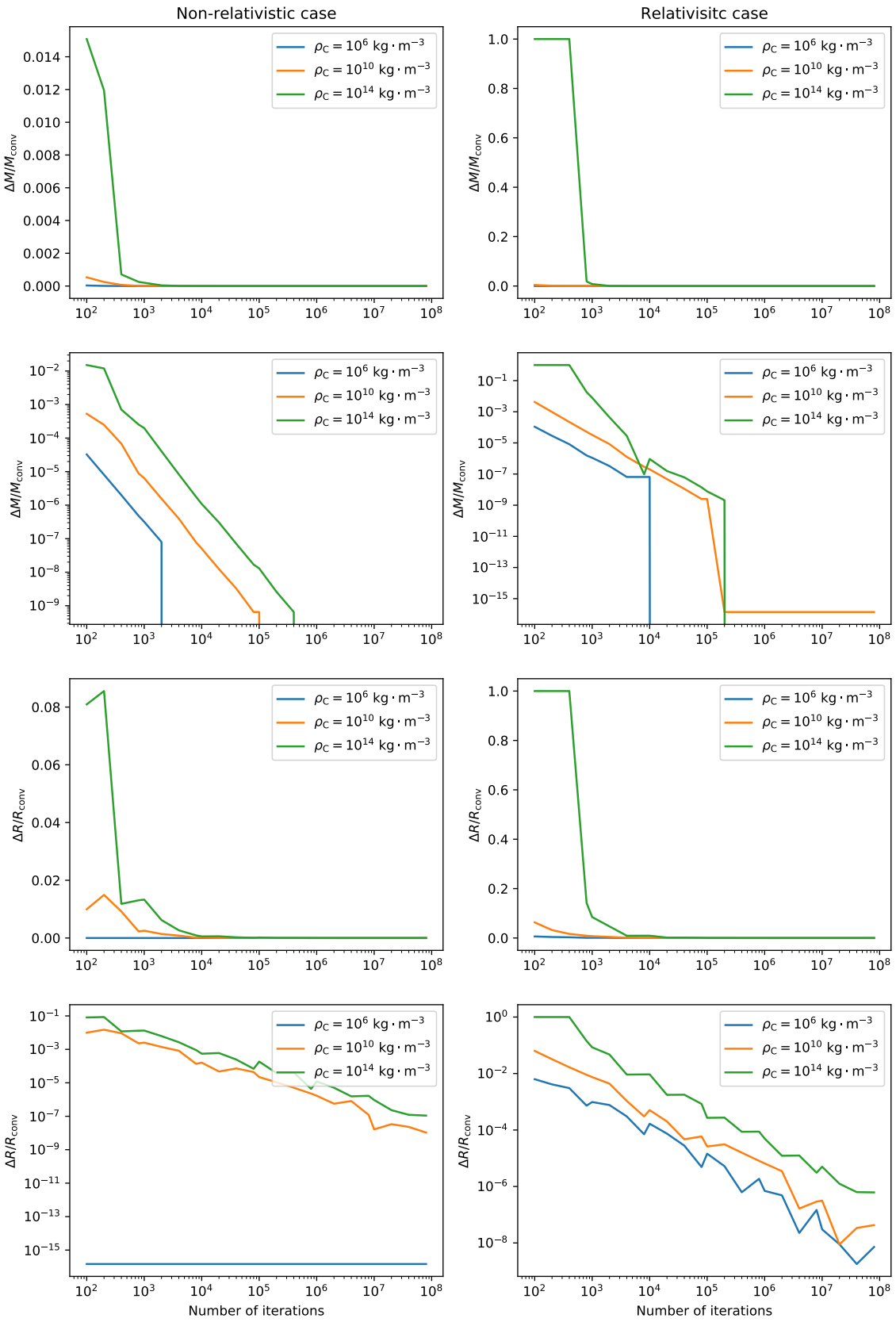

Figure 2: Plot of convergence for three central spanning the tested range of ρ_c in both non-relativistic (left column) and relativistic (right column) cases. As can be seen, convergence is slower in the relativistic case; after 10^6 intervals good accuracy is achieved in both cases for both mass and radius values. The values $M_{\text{conv}}, R_{\text{conv}}$ are computed as the average of the last three values; $\Delta M = |M - M_{\text{conv}}|$ and $\Delta R = |R - R_{\text{conv}}|$. Odd rows have a linear y-axis, even rows are the same plot with a logarithmic y-axis.